Am J Physiol Endocrinol Metab 291: E704–E715, 2006.
First published May 16, 2006; doi:10.1152/ajpendo.00048.2006.

Differential coupling of β_{3A}- and β_{3B}-adrenergic receptors to endogenous and chimeric $G_\alpha s$ and $G_\alpha i$

Natalie R. Lenard,[1,*] Veronica Prpic,[1,*] Aaron W. Adamson,[1] Richard C. Rogers,[2] and Thomas W. Gettys[1]

Laboratories of [1]Adipocyte Signaling and [2]Autonomic Neuroscience, Pennington Biomedical Research Center, Baton Rouge, Louisiana

Submitted 1 February 2006; accepted in final form 8 May 2006

Lenard, Natalie R., Veronica Prpic, Aaron W. Adamson, Richard C. Rogers, and Thomas W. Gettys. Differential coupling of β_{3A}- and β_{3B}-adrenergic receptors to endogenous and chimeric $G_\alpha s$ and $G_\alpha i$. *Am J Physiol Endocrinol Metab* 291: E704–E715, 2006. First published May 16, 2006; doi:10.1152/ajpendo.00048.2006.— Chimeric G proteins made by replacing the COOH-terminal heptapeptide of $G_\alpha q$ with the COOH-terminal heptapeptide of $G_\alpha s$ or $G_\alpha i$ were used to assess the relative coupling of β_3-adrenergic receptor (β_3-AR) splice variants (β_{3A} and β_{3B}) to $G_\alpha s$ and $G_\alpha i$. The $G_\alpha q/s$ and $G_\alpha q/i$ chimeras transformed the response to receptor activation from regulation of adenylyl cyclase to mobilization of intracellular calcium ($Ca^{2+}{}_i$). Complementary high-throughput and single-cell approaches were used to evaluate agonist-induced coupling of the receptor to the G protein chimeras. In cells stably transformed with rat β_3-AR, transfected with the G protein chimeras, and evaluated using a scanning fluorometer, β_3-AR-induced coupling to $G_\alpha q/s$ produced a rapid eightfold increase in $Ca^{2+}{}_i$ followed by a slow decay to levels 25% above baseline. $G_\alpha q/i$ also linked rat β_3-AR to mobilization of $Ca^{2+}{}_i$ in a similar time- and agonist-dependent manner, but the net 2.5-fold increase in $Ca^{2+}{}_i$ was only 30% of the response obtained with $G_\alpha q/s$. Activation of the rat β_3-AR also increased GTP binding to endogenous $G_\alpha i$ threefold in membranes from CHO cells stably transformed with the receptor. A complementary single-cell imaging approach was used to assess the relative coupling of mouse β_{3A}- and β_{3B}-AR to $G_\alpha i$ under conditions established to produce equivalent agonist-dependent coupling of the receptor splice variants to $G_\alpha q/s$ and to increases in intracellular cAMP through endogenous $G_\alpha s$. The β_{3A}- and β_{3B}-AR coupled equivalently to $G_\alpha q/i$, but the temporal patterns of $Ca^{2+}{}_i$ mobilization indicated that coupling was significantly less efficient than coupling to $G_\alpha q/s$. Collectively, these findings indicate less efficient but equivalent coupling of β_{3A}- and β_{3B}-AR to $G_\alpha i$ vs. $G_\alpha s$ and suggest that differential expression of the splice variants would not produce local differences in signaling networks linked to β_3-AR activation.

β-adrenergic receptor; G proteins; cyclic adenosine monophosphate; signaling plasticity

β-ADRENERGIC RECEPTORS (β-AR) belong to the superfamily of 7-transmembrane-domain G protein-coupled receptors that increase intracellular cAMP by coupling to and activating $G_\alpha s$, but β_3-ARs are distinct from classical β_1- and β_2-AR in many ways. Pharmacological studies demonstrate that β_3-ARs are either poorly antagonized by (e.g., propranolol) or partially activated by (e.g., CGP 12177A, pindolol) conventional nonselective and β_1/β_2-AR antagonists (26). Another important difference is that β_1/β_2-ARs are subject to desensitization, which occurs by phosphorylation of serines and threonines in the intracellular COOH-terminal tail by G protein receptor kinase (GRK) and phosphorylation of the third intracellular loop by PKA (2, 29). However, the β_3-AR has fewer serine and threonine residues in the COOH-terminal tail and lacks the consensus PKA target sequence in the third intracellular loop (12). PKA-dependent phosphorylation of this region in β_1/β_2-ARs reduces their affinity for $G_\alpha s$ and increases their affinity for $G_\alpha i$, resulting in the "switch" that is observed following chronic agonist stimulation of β_1/β_2-ARs (10). These structural differences limit posttranslational regulation of the β_3-AR and make it less sensitive to agonist-induced desensitization (30).

Unlike the β_1/β_2-ARs, the β_3-AR contains introns (21). Alternative splicing generates two splice variants of the mouse β_3-AR (β_{3A}-AR and β_{3B}-AR) that differ in their COOH-terminal tails (13). Interestingly, the β_{3B}-AR has two additional serine residues in its COOH-terminal tail. A recent study reported that mutating these residues to alanine had no effect on receptor binding to the antagonist ^{125}I-cyanopindolol (ICYP) but completely blocked agonist-dependent increases in cAMP (39). Although it is unclear whether the receptor is regulated by phosphorylation of these serines (Ser^{388} and Ser^{389}), these and previous findings (23) indicate that the COOH termini of β_3-ARs are important for functional coupling to G proteins. The two β_3-AR splice variants share a common pharmacology but differ in their tissue distribution. The β_{3A}-AR is the predominant isoform among tissues studied to date (13). Highest levels of the less common β_{3B}-AR are found in hypothalamus, cortex, and white adipose tissue (WAT), whereas the lowest levels are found in the ileum and brown adipose tissue (BAT) (13). The β_{3B}-AR makes up ~21% of total β_3-AR mRNA in WAT, whereas the β_{3B}-AR comprises only 7% of total β_3-AR mRNA in BAT (13).

The significance of differential expression of the β-AR splice variants is inferred from previous studies showing that the β_3-AR is capable of coupling to and activating $G_\alpha i$ (4, 40), and recent work from Hutchinson et al. (23) reporting that the β_{3B}-AR, but not the β_{3A}-AR, can activate $G_\alpha i$. Thus differences in expression of β_{3B}-AR splice variants between BAT and WAT could lead to activation of dual signals in WAT ($G_\alpha s$ and $G_\alpha i$), whereas in BAT, signaling would occur primarily through $G_\alpha s$. If correct, this could produce tissue-specific differences in translation of sympathetic input. However, the findings of differential coupling of β_3-AR splice variants to $G_\alpha i$ were based on experiments using pertussis toxin (PTX) to

* These two authors contributed equally to this work.

Address for reprint requests and other correspondence: T. W. Gettys, 6400 Perkins Rd., Pennington Biomedical Research Center, Baton Rouge, LA 70808 (e-mail: gettystw@pbrc.edu).

The costs of publication of this article were defrayed in part by the payment of page charges. The article must therefore be hereby marked "*advertisement*" in accordance with 18 U.S.C. Section 1734 solely to indicate this fact.

inactivate receptor coupling to $G_\alpha i$ (23). PTX pretreatment increased the maximal cAMP response to CL-316243 in cells transfected with the β_{3B}-AR, but not in cells transfected with the β_{3A}-AR, leading the authors to conclude differential coupling of the receptor splice variants to $G_\alpha i$. PTX has been shown to have a number of signaling effects that are independent of ADP ribosylation of $G_\alpha i$, such as activation of ERK1/2 (15), tyrosine kinases (28), Toll-like receptor 4 (25), and NF-κB (24). These and other $G_\alpha i$-independent effects of PTX affect signaling crosstalk, cell morphology, and cell function and have the potential to confound interpretation of receptor-G protein interactions based on downstream readouts. To assess relative coupling of β_3-AR splice variants to $G_\alpha s$ and $G_\alpha i$ in the absence of PTX, two experimental approaches were used. The first approach used a cross-linkable analog of GTP to measure receptor-dependent binding of GTP by $G_\alpha i$ (16), and the second approach used chimeric G proteins developed by Conklin and colleagues (7, 8) and Coward et al. (9). The G protein chimeras, prepared by replacing the COOH-terminal heptapeptide of $G_q\alpha$ with the COOH terminus of $G_\alpha s$ or $G_\alpha i$, transform the response to receptor-dependent G protein activation from regulation of adenylyl cyclase to mobilization of intracellular calcium ($Ca^{2+}{}_i$). Using Chinese hamster ovary (CHO) cells transfected with β_3-AR splice variants and the respective approaches, we find that β_{3A}-AR and β_{3B}-AR couple equivalently to $G_\alpha i$ but ~70% less effectively than they couple to $G_\alpha s$.

MATERIALS AND METHODS

Materials. All tissue culture reagents other than fetal bovine serum (Hyclone, Logan, UT) were from Invitrogen (Carlsbad, CA). Fugene 6 was purchased from Roche (Indianapolis, IN). Fluo 3-AM was from Molecular Probes (Carlsbad, CA), and the FLIPR calcium assay kit was from Molecular Devices (Sunnyvale, CA). All other reagents were from Sigma-Aldrich (St. Louis, MO). The β_3-AR agonist CL-316243 was a gift from Dr. Kurt Steiner at Wyeth Ayerst (Monmouth Junction, NJ). The GTP photoaffinity probe, 4-azidoanilido-[α-^{32}P]GTP (AA-GTP), was obtained from ALT (Lexington, KY). The mouse monoclonal HA antibody (clone 12CA5) was obtained from Roche (San Diego, CA). The ^{125}I-labeled cAMP-tyrosyl methylester (TME) was prepared by iodination of cAMP-TME and purification of labeled from unlabeled ligand by C_{18} reverse-phase HPLC as previously described (17).

Cell culture. CHO-K1 cells were obtained from American Type Culture Collection (Manassas, VA) and maintained in F-12 K medium supplemented with 10% (vol/vol) FBS, 1% penicillin (100 U/ml), and streptomycin (100 mg/ml) at 37°C in a humidified 5% CO_2 atmosphere. The CHO cells used for study never exceeded passage 20. CHO cells stably transformed with the M1 muscarinic receptor (M1-CHO) were cultured in Ham's F-12 medium supplemented with 10% FBS, glutamine, penicillin, and streptomycin and 50 μg/ml G418 at 37°C in a humidified 5% CO_2 atmosphere.

Plasmids. The expression construct for the rat β_3-AR was provided by Dr. James Granneman (Wayne State University, Detroit, MI). The expression constructs for the mouse β_{3A}-AR and β_{3B}-AR were provided by Dr. Roger Summers (Monash University, Victoria, Australia), and the expression constructs for HA-tagged $G_\alpha q$/s and $G_\alpha q$/i chimeras were provided by Dr. Bruce Conklin (Gladstone Institute, University of California, San Francisco, CA). CHO cells stably transformed with the serotonin (5-HT_{1A}) receptor were provided by Dr. John Raymond (Medical University of South Carolina, Charleston, SC). The inserts for the rat β_3-AR, mouse β_{3A}- and β_{3B}-AR were subcloned into the pcDNA 3.1 expression vector (Invitrogen) by standard molecular biology techniques and confirmed by sequencing. The plasmid expressing the reef coral (*Discosoma sp.*) red fluorescent protein (DsRed) was obtained from BD Pharmogen (Mountain View, CA).

Preparation of CHO cells stably expressing rat β_3-AR. A CHO cell line stably transformed with M1 CHO was provided as a positive control by Molecular Devices (Sunnyvale, CA) and used with their Fluorometric Imaging Plate Reader with Integrated Fluidics (FLEX Station) to measure agonist-dependent mobilization of intracellular calcium ($Ca^{2+}{}_i$). The M1 receptor couples to endogenous $G_q\alpha$ and mobilizes $Ca^{2+}{}_i$ through activation of phospholipase C. CHO cells stably transformed with the rat β_3-AR were prepared by transfecting the β_3-AR into CHO cells with Lipofectamine (Invitrogen) according to the manufacturer's instructions. G-418 was used as the selection agent (500 μg/ml) for 3 wk, and selected clones were screened and selected on the basis of β_3-AR agonist-dependent increases of intracellular cAMP. Selected clones were maintained in G-418 (50 μg/ml).

Agonist-dependent coupling of rat β_3-AR to endogenous $G_\alpha i$. To measure directly whether the rat β_3-AR could activate endogenous $G_\alpha i$ in our cell line, CHO cell plasma membranes from cells stably expressing the rat β_3-AR or human 5-HT_{1A} receptor were prepared by differential centrifugation and incubated with 0.5 μCi of 4-azidoanilido-[α-^{32}P]GTP (AA-GTP) and 3 μM GDP in the presence or absence of 1 μM CL-316243 (rat β_3-AR) or 1 μM serotonin (human 5-HT_{1A} receptor) for 3 min as previously described (16, 37). Thereafter, the membranes were collected, and bound AA-GTP was cross-linked to $G_\alpha i$ proteins under UV light (254 nm) for 3 min at 4°C. Proteins were resolved by SDS-PAGE, visualized on film, and quantitated by scanning densitometry to assess receptor-dependent $G_\alpha i$ activation (16).

Measurement of rat β_3-AR coupling to G protein chimeras with FLEX Station. For automated calcium measurements using the FLEX Station, initial studies were conducted with CHO cells stably transformed with M1 muscarinic receptor, which couples to endogenous $G_q\alpha$ and mobilizes $Ca^{2+}{}_i$ through activation of phospholipase C. The M1 cell line served as a positive control to establish assay conditions and validate the method. Thereafter, CHO cells stably transformed with M1 receptor or the rat β_3-AR were plated overnight at a seeding density of 2.2×10^6/100-mm dish. The following day, CHO cells from the β_3-AR line were transiently transfected with the $G_\alpha q$/s or $G_\alpha q$/i chimeras, or vector alone using Fugene 6 (3 μg cDNA/100-mm dish). In initial experiments, CHO cells expressing the β_3-AR were also cotransfected with an expression construct for the red fluorescent protein DsRed and evaluated by fluorescence microscopy at 600 nm to evaluate transfection efficiency (~45%) and confirm equal efficiency between cells transfected with each G protein chimera. After 24 h, cells were detached and split using trypsin-EDTA (0.5 mM) and seeded on polylysine-coated 96-well black-walled plates at a density of 80,000 cells/well. Plated cells were loaded with Molecular Device's FLIPR calcium assay kit for 90 min at 37°C according to the manufacturer's instructions. Without being washed, the plates were placed in the FLEX Station, and its integrated fluidics were used to add buffer to lift loose cells first, establish a stable baseline recording, and then add the desired concentration of the respective agonist for each cell type. Carbachol was used for the M1-CHO line, and CL-316243 was used for the β_3-AR line. The excitation fluorescence was 485 nm, and the emission fluorescence was 520 nm using a 515-nm emission cutoff filter. Seven individual fields on the bottom of each well were set for the fluorescence path measurement. Agonist-dependent changes in fluorescence were recorded and exported to GraphPad Prism (San Diego, CA) for analysis of kinetic parameters.

Transient transfection of β_{3A}- and β_{3B}-AR and G protein chimeras for single-cell fluorescense microscopy. CHO cells were seeded at a density of 20,000 cells/6-well plate in F-12 K medium described above and incubated overnight at 37°C in a humidified 5% CO_2 atmosphere. The following day, cells were cotransfected with the indicated combination of expression constructs (2.4 μg of total

cDNA) and Fugene 6 in a 1:3 ratio according to manufacturer's instructions for 24 h. To positively identify transfected cells for study, the expression construct for red fluorescent protein DsRed was included during cotransfection with the receptor and G protein constructs. The cells that were positive for DsRed were identified and analyzed by fluorescence microscopy. The DsRed was chosen because it has an excitation/emission spectrum distinct from the probe (Fluo 3) used for measurement of changes in intracellular calcium.

The cells were evaluated 16 h after transfection by placing them in 1 ml of the F-12 K medium without serum but containing 10 mM HEPES, pH 7.4, 1 mM probenecid, and 10 μM Fluo 3-AM for 30–45 min at room temperature in the dark. The cells were washed three times with Hanks' buffered salt solution supplemented with 10 mM HEPES, pH 7.4 (HHBSS), and placed in 1.9 ml of HHBSS. Culture dishes were then mounted onto the microscope stage (Nikon), and DsRed-expressing cells were identified for analysis. Fluo 3 fluorescence was measured in these cells by use of an excitation filter of 495 nm on the selection illuminator (Illuminator D6), an emitter of 520 nm, and a low light camera (Photometrics) interfaced with the microscope and controlled by Metamorph software. For time lapse fluorescence measurements, cells chosen for further analysis were well distanced from one another and uniformly loaded with Fluo 3. The stability of the fluorescence background was checked with the addition of 50 μl of HHBSS buffer. Evaluation of receptor coupling to mobilization of $Ca^{2+}{}_i$ through the G protein chimeras was initiated by addition of agonists (50 μl) and monitored through time using Metamorph software. The relative changes in $[Ca^{2+}]_i$ were measured as changes in fluorescence (F), where F is the fluorescence intensity of an area of interest (i.e., within DsRed-expressing cells) before stimulation (denoted as 100%), and ΔF is the change from this value during the time course of stimulation. Background fluorescence (from a designated area without Fluo 3-loaded cells) was subtracted from the fluorescence of the Fluo 3-loaded cells before calculations were performed. Numerical fluorescence data were exported to Graphpad Prism for calculation of the following kinetic parameters: maximum fluorescence, duration of peaks, and frequency of peaks per 5 min of measurements. These variables were analyzed to compare relative coupling of β_{3A}-AR and β_{3B}-AR to the $G_\alpha q/s$ and $G_\alpha q/i$ chimeras.

Measurement of intracellular cAMP. Cells from selected experiments were preincubated for 5 min with 100 μM IBMX and stimulated for 10 min with 10 μM CL-316243. The reaction was stopped with ice-cold TCA (2.5% final concentration). The supernatants were transferred into Eppendorf tubes and centrifuged, and cAMP was measured in the clear supernatants by radioimmunoassay as described previously (17).

Measurement of adenylyl cyclase activity. Crude membranes were prepared from CHO cells transfected for 48 h with either the β_{3A}-AR or β_{3B}-AR as previously described (16, 38). The membranes were resuspended at 1 mg/ml in 25 mM HEPES (pH 7.4) containing 140 mM NaCl, 40 μM leupeptin, 1 μg/ml soybean trypsin inhibitor, and 1 mM EDTA and snap-frozen with liquid nitrogen in 100-μg aliquots for subsequent measurement of adenylyl cyclase and receptor binding to ^{125}I-cyanopindolol (ICYP). Adenylyl cyclase activity was measured by incubating 10-μg aliquots of membranes from each receptor preparation for 10 min at 30°C in a buffer containing 50 mM TES (pH 7.4), 4 mM $MgCl_2$, 2 mM creatine phosphate, 25 U/ml creatine phosphokinase, 100 μM ATP, 10 μM GTP, and incremental concentrations of CL-316243 as previously described (17). The reaction was stopped with ice-cold TCA, and cAMP formed in the reaction was measured as before (17). Dose response curves were characterized using the four-paramater logistic ogive in relation to log dose as described previously (19).

Measurement of ICYP binding. Radioligand binding assays were conducted with membranes from CHO cells transfected with β_{3A}-AR or β_{3B}-AR by incubating membranes from each source (10–15 μg) with 40 pM ICYP in 25 mM HEPES (pH 7.4) containing 12.5 mM $MgCl_2$ for 1 h at 37°C, as described previously (5). Bound ICYP was collected on filters in a Skatron cell harvester (Molecular Devices), and counts per minute of bound ICYP were converted to femtomoles of ICYP bound based on the specific activity of the ICYP used (2,200 Ci/mmol).

Measurement of $G_\alpha q/s$ and $G_\alpha q/i$ expression. Whole cell extracts were prepared from CHO cells cotransfected with $G_\alpha q/s$ or $G_\alpha q/i$, and the β_3-AR expression vector and $G_\alpha q/s$ and $G_\alpha q/i$ expression were measured in 200-μg aliquots from each chimera. Identical whole cell extracts from cells cotransfected with empty vector and β_3-AR expression vector were used as a negative control. The blots were probed with 12CA5 monoclonal HA antibody and visualized by standard ECL procedure. Band intensity was quantitated by densitometry using the Versadoc system (Bio-Rad).

Methods of analysis. The agonist-dependent increases in cAMP for each receptor/G protein chimera combination were compared using a two-way analysis of variance, with post hoc testing of group means using the Bonferroni correction. Specific binding of ICYP in membranes from CHO cells transfected with empty vector or β_{3A}-AR or β_{3B}-AR expression constructs was compared by one-way analysis of variance. To compare the ability of the rat β_3-AR to couple to $G_\alpha q/s$ vs. $G_\alpha q/i$, maximal agonist-dependent increases in $[Ca^{2+}]_i$ measured with the FLEX Station were compared using a one-tailed *t*-test ($\alpha = 0.05$). The relative coupling of mouse β_{3A}-AR and β_{3B}-AR to $G_\alpha q/s$ vs. $G_\alpha q/i$ was measured using fluorescence microscopy and evaluated by comparing the patterns of agonist-induced $Ca^{2+}{}_i$ mobilization produced by each receptor/G protein pair. The magnitude, duration, and frequency/unit time of $Ca^{2+}{}_i$ oscillations produced by agonist were calculated from each recording and compared using two-way analysis of variance. A one-way analysis of variance was used to compare receptor-dependent binding of AA-GTP to endogenous $G_\alpha i$ and to compare ICYP binding in membranes from cells transfected with the β_{3A}-AR or β_{3B}-AR. Post hoc testing of group means was made using the pooled error term to calculate standard errors. Protection against type I errors was set at 5% ($\alpha = 0.05$).

RESULTS

Sequence differences between rat and mouse β_3-AR. Amino acid sequences of the rat β_3-AR (20) and mouse β_{3A}-AR and β_{3B}-AR (13) splice variants used herein are presented in Fig. 1. The first 387 amino acids of the mouse β_{3A}- and β_{3B}-AR are identical, but the β_{3B}-AR has a unique COOH terminus (SSLLREPRHLYTCLGYP) that is four residues longer and completely distinct from the COOH terminus of the mouse β_{3A}-AR (RFDGYEGARPFPT). Compared with the mouse β_3-AR, the first 387 residues of the rat β_3-AR contain 21 amino acid substitutions, and, as shown in Fig. 1, the majority are conservative changes. This translates into 95.4% homology between the rat β_3-AR and the mouse β_3-AR splice variants in this region of the protein. Interestingly, the COOH terminus of the rat β_3-AR is identical to that of the mouse β_{3A}-AR except for a nonconservative substitution of glutamic acid for alanine at position 395 (Fig. 1). Thus the similarities and differences among the three receptors provide an initial basis for evaluating the role of specific sequences in differential coupling of the β_3-AR to G protein subtypes.

Coupling of transfected rat and mouse β_3-ARs to endogenous $G_\alpha s$ and $G_\alpha i$. To confirm that transfected β_3-AR receptors were biologically active and to establish conditions of equivalent functional expression for the various studies, initial experiments were conducted with stably transformed CHO cells expressing the rat β_3-AR and CHO cells transiently transfected with mouse β_3-AR splice variants and G protein chimeras. In the first of two sets of experiments conducted with the stably

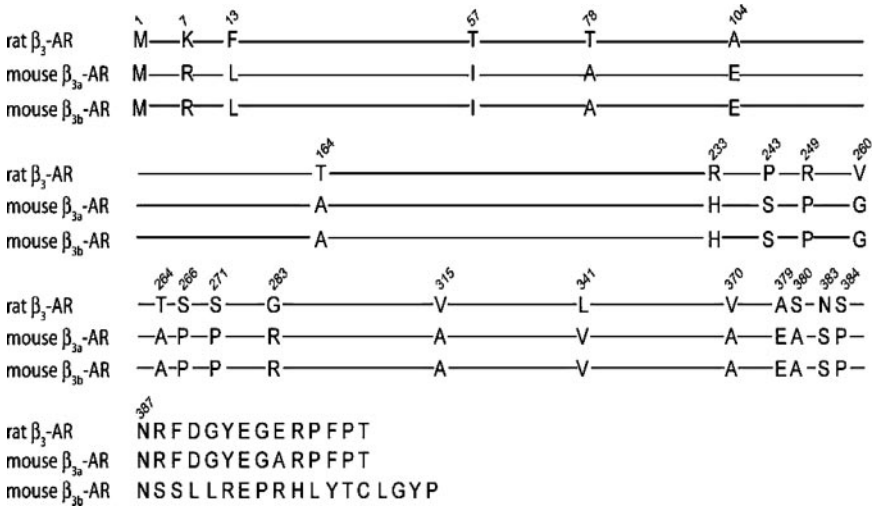

Fig. 1. Amino acid sequence alignment of rat β_3-AR (adrenergic receptor), mouse β_{3A}-AR, and β_{3B}-ARs. The first 387 amino acids of the mouse β_3-AR isoforms are identical. The 21 amino acid substitutions in the rat β_3-AR sequence are identified, which translates to 95.4% homology between rat and mouse β_3-ARs in this region. Mouse β_{3B}-AR has a unique COOH terminus with 17 amino acids (SSLLREPRHLYTCLGYP), which is distinct from the COOH-terminal 13-amino acid sequence (RFDGYEGARPFPT) of the mouse β_{3A}-AR. Rat β_3-AR and mouse β_{3A}-AR COOH-terminal sequences are identical, except for a glutamic acid-for-alanine substitution at position 395.

transformed rat β_3-AR line, the cells were transiently transfected with empty vector or vectors for $G_\alpha q/s$ or $G_\alpha q/i$, followed by measurement of agonist-dependent increases in intracellular cAMP. Basal cAMP concentration was similar in each line (empty vector 1.85 ± 0.15, $G_\alpha q/s$ 1.04 ± 0.13, $G_\alpha q/i$ 2.14 ± 0.14 pmol/well), and a 10-min incubation with the β_3-AR agonist CL-316243 (10 μM) produced similar increases in intracellular cAMP in each group (empty vector 6.51 ± 1.08, $G_\alpha q/s$ 5.69 ± 0.86, $G_\alpha q/i$ 6.47 ± 0.73 pmol/well). These results provide no evidence that transient transfection of G protein chimeras affects functional coupling of the rat β_3-AR to endogenous $G_\alpha s$. They also provide a common basis for comparing the relative coupling of the rat β_3-AR to the $G_\alpha q/s$ and $G_\alpha q/i$ chimeras. In the second set of experiments, incubation of plasma membranes from this cell line with the photo-cross-linkable GTP analog AA-GTP and receptor agonist (1 μM CL-316243) produced a threefold increase in binding of AA-GTP to proteins migrating at 40–41 kDa (Fig. 2). AA-GTP binding was not increased by CL-316243 in plasma membranes from cells transformed with empty vector, but in membranes from cells expressing the canonical $G_\alpha i$-coupled receptor 5-HT_{1A}, the receptor agonist (serotonin) produced a five- to sixfold increase in AA-GTP binding to a 41-kDa band (Fig. 2) that we previously showed (16) by immunoprecipitation to contain both $G_\alpha i$-2 and $G_\alpha i$-3. Collectively, these findings indicate that the rat β_3-AR couples to endogenous $G_\alpha i$ in an agonist-dependent manner and that transient transfection of G protein chimeras does not affect receptor coupling to endogenous $G_\alpha s$.

Similar control experiments were run with CHO cells transiently transfected with the mouse β_3-AR splice variants and G protein chimeras. In this case, it was essential to obtain equivalent functional receptor expression between CHO cells transfected with β_{3A}-AR vs. β_{3B}-AR so that differences in G protein coupling could be properly attributed to differences in receptor sequence rather than expression. And as addressed above, it was also important to establish that cotransfection with the G protein chimeras did not selectively alter receptor function. By use of basal and agonist-induced increases in cAMP as end points, two-way analysis of variance provided no evidence of an interaction between receptor splice variant and G protein chimera with either response variable (Fig. 3, *A* and *B*). Post hoc testing of group means confirmed that cotransfection of $G_\alpha q/s$ or $G_\alpha q/i$ had no effect on basal or agonist-induced cAMP with either receptor splice variant (Fig. 3, *A* and *B*). In addition, the CL-316243-induced increases in intracellular cAMP did not differ between CHO cells transfected with β_{3A}-AR vs. β_{3B}-AR, regardless of G protein chimera (Fig. 3, *A* and *B*). Collectively, these findings support the conclusion that transient transfection of the receptor splice variants using our protocol produced equivalent functionality with respect to agonist-dependent increases in cellular cAMP.

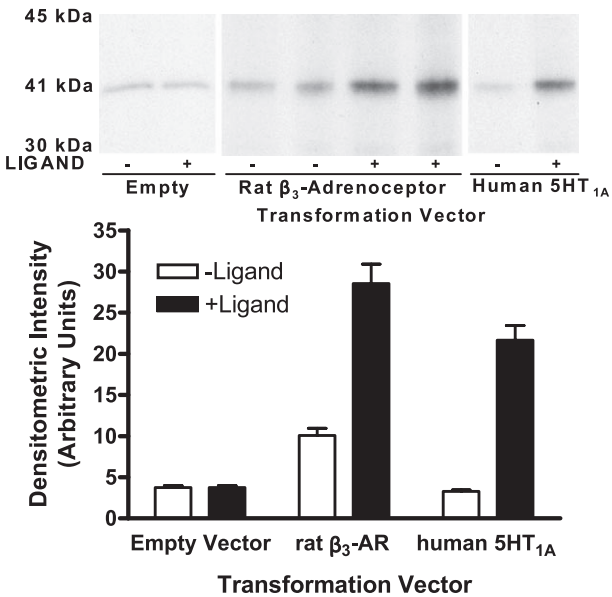

Fig. 2. Functional coupling of rat β_3-AR to endogenous $G_\alpha i$. Plasma membranes (40 μg) from Chinese hamster ovary (CHO) cells stably expressing rat β_3-AR, empty vector, or human 5-HT_{1A} (serotonin) receptor were incubated with 0.5 μCi of 4-azidoanilido-[α-^{32}P]GTP in the presence or absence of 1 μM CL-316243 (empty vector and rat β_3-AR) or 1 μM 5-HT_{1A} for 3 min, as described in MATERIALS AND METHODS. Thereafter, membranes were collected, and bound GTP photolabel was cross-linked to proteins under UV light and resolved by SDS-PAGE. Intensity of ligand-dependent labeling of proteins migrating at 41 kDa ($G_\alpha i$) was visualized on film and quantitated by scanning densitometry. Autoradiogram is representative of 3 replicates of this experiment.

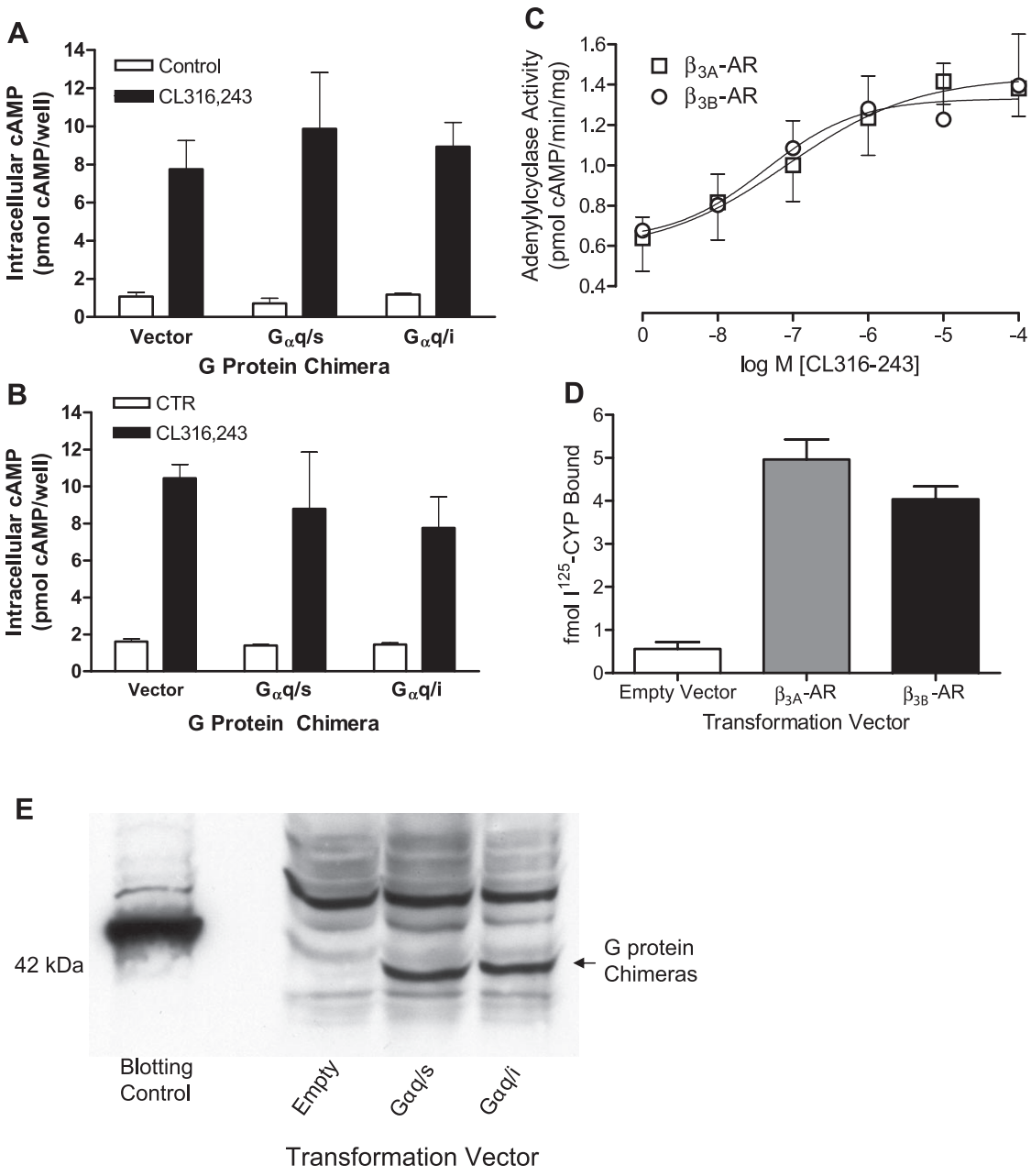

Fig. 3. Expression and function of mouse β_{3A}-AR and β_{3B}-AR in CHO cells (*A* and *B*) and CHO cell membranes (*C* and *D*). *E*: expression of G protein chimeras in CHO cells. *A* and *B*: CHO cells were transiently transfected with mouse β_{3A}-AR (*A*) or mouse β_{3B}-AR (*B*) along with empty vector or $G_\alpha q/s$ or $G_\alpha q/i$ chimeras, and β_3-AR agonist-dependent increases in intracellular cAMP were measured. Cells were preincubated for 5 min with 100 μM IBMX and treated for 10 min with the β_3-AR agonist CL-316243 (10 μM). The reaction was stopped with ice-cold TCA (2.5% final concentration), transferred to Eppendorf tubes, and microcentrifuged for 7 min at full speed. cAMP was assayed in dilutions of clear supernatant using RIA, as described in MATERIALS AND METHODS. Means ± SE from triplicate determinations in each of 2 experiments were analyzed by ANOVA. *C*: CHO cells were transiently transfected with mouse β_{3A}-AR, β_{3B}-AR, or empty vector and crude membranes prepared from each transfection for assessment of agonist-dependent adenylyl cyclase activation (*C*) or receptor-binding studies (*D*). Membranes from CHO cells transfected with either β_{3A}-AR or β_{3B}-AR were incubated with increasing concentrations of CL-316243, and the cAMP formed in the reaction was measured as described in MATERIALS AND METHODS. Response curves were fitted by least squares, and parameter estimates for potency and efficacy were used to compare responses of each receptor isoform. Original observations and fitted curves are representative of 3 separate experiments. *D*: membranes from CHO cells transfected with empty vector, β_{3A}-AR, or β_{3B}-AR were incubated with 40 pM ^{125}I-cyanopindolol (ICYP) in the presence and absence of a saturating concentration of isoproterenol (100 μM) for 1 h at 37°C, as described in MATERIALS AND METHODS. Specific binding of ICYP to receptor isoforms was determined after filtration, and means ± SE from duplicate determinations in each of 2 experiments were analyzed by ANOVA. *E*: whole cell extracts were prepared from CHO cells cotransfected with β_3-AR expression vector and $G_\alpha q/s$, $G_\alpha q/i$, or empty vector, as described in MATERIALS AND METHODS. Aliquots (200 μg) of each extract were resolved by SDS-PAGE, and after electrophorectic transfer to nitrocellulose membranes, blots were probed with monoclonal anti-HA antibody (12CA5). Detected bands were visualized by ECL and quantitated by densitometry for comparison by *t*-test. Blot is representative of 3 separate experiments.

Comparison of β_{3A}-AR or β_{3B}-AR activation of adenylyl cyclase. Functional coupling of transfected β_{3A}- and β_{3B}-ARs to adenylyl cyclase was also assessed in membranes from CHO cells transfected with each receptor isoform. This approach provided a second method to evaluate relative expression of the receptor isoforms in cells transfected with each expression construct. Incubation of each membrane preparation with the β_3-AR-selective agonist CL-316243 produced comparable concentration-dependent activation of adenylylcylase with each receptor isoform (Fig. 3*C*). Estimates of potency (β_{3A}-AR 85.0 ± 9.1 and β_{3B}-AR 43.2 ± 8.9 nM) and efficacy (β_{3A}-AR 1.44 ± 0.19 and β_{3B}-AR 1.33 ± 0.14 pmol·min^{-1}·mg^{-1}) from the fitted curves did not differ between receptor isoforms (Fig. 3*C*). These findings complement our findings in intact cells (Fig. 3, *A* and *B*) and further support the conclusion of equivalent functionality of the transfected receptor isoforms.

Comparison of β_{3A}-AR or β_{3B}-AR binding to ICYP. The membranes used to measure adenylyl cyclase activation were also used to assess the respective binding of the receptor isoforms to ICYP. Binding of ICYP was compared at 40 pM ICYP, which is ~20-fold lower than the estimated dissociation constant (880 ± 90 pM) of ICYP for the mouse β_3-AR (35). This concentration provides a sensitive test for differences in receptor density between preparations. As expected, specific ICYP binding was not detected in membranes from cells transfected with empty vector (Fig. 3*D*). Figure 3*D* also suggests slightly higher ICYP binding in the β_{3A}-AR vs. β_{3B}-AR membrane preparations, but analysis of variance provided no evidence that the means were different ($P > 0.05$). Collectively, the results presented in Fig. 3, *A–D*, show comparable expression of the β_3-AR isoforms, using our transfection protocol, and establish a common basis for comparing their coupling to G protein chimeras in subsequent experiments.

Comparison of G protein chimera expression. Finally, whole cell extracts from CHO cells transiently transfected with the β_3-AR expression vector and the G_αq/s or G_αq/i expression constructs were used to examine the relative expression of the G protein chimeras by Western blotting. The G protein chimeras were detected via an internal HA epitope tag, and Fig. 3*E* shows that expression of the G protein chimeras was not detected in cells transfected with empty vector and that the respective G protein chimeras were expressed at similar levels in CHO cells transfected with each chimera. Endogenous G_αq, G_αs, and G_αi expressions were also compared between the CHO cells transfected with each chimera and the CHO cells transfected with empty vector. We found no evidence that endogenous G protein expression was altered by the G protein chimeras (data not shown). Considered together, these findings establish that comparisons of receptor-G protein coupling are based on comparable expression of the β_3-AR isoforms and the G protein chimeras, providing a common basis for comparing coupling efficiency of the β_3-AR isoforms to the respective G protein chimeras.

Comparison of rat β_3-AR coupling to G_αs vs. G_αi. Initial control experiments were conducted with CHO cells stably expressing the M1-CHO or the rat β_3-AR. The M1-CHO couples to endogenous G_αq and was used as a positive control to optimize Ca^{2+}-sensitive probe loading and receptor-dependent mobilization of $Ca^{2+}{}_i$. Initial experiments showed that baseline fluorescence was stable and not affected by addition of buffer to either M1-CHO or rat β_3-AR CHO. However, addition of 1 μM carbachol produced a rapid increase of ~15,000 relative fluorescence units above baseline in M1-CHO cells (Fig. 4). In contrast, addition of CL-316243 to β_3-AR-expressing CHO cells had no effect on $Ca^{2+}{}_i$ (Fig. 4), indicating that the β_3-AR does not couple to endogenous $G_q\alpha$. This control experiment also established that the β_3-AR does not alter $Ca^{2+}{}_i$ through its coupling to G_αs or G_αi. Carbachol had no effect on $Ca^{2+}{}_i$ in β_3-AR CHO or untransfected CHO cells (not shown).

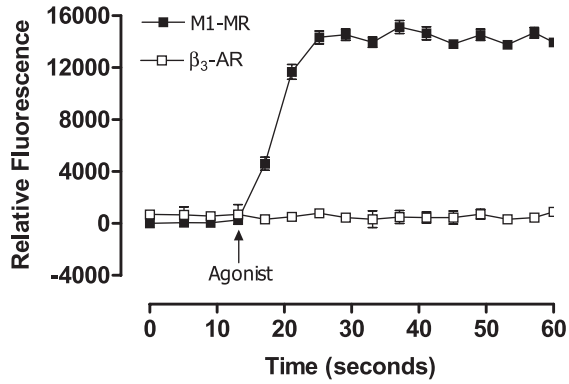

Fig. 4. Receptor-dependent mobilization of intracellular calcium ($Ca^{2+}{}_i$) in CHO cells stably transformed with the M1 muscarinic receptor (■) or the rat β_3-AR (□). Cells from each line were plated onto 96-well black plates at a seeding density of 80,000 cells/well. Next morning, cells were preloaded for 90 min with the FLIPR calcium assay kit. Plates were placed in the 37°C chamber of the FLEX Station, and stable baseline recordings were obtained as described in MATERIALS AND METHODS. Excitation fluorescence was 485 nm and emission was detected at 520 nm with 515-nm emission cutoff filter. Buffer control and M1 muscarinic agonist carbachol (10 μM) or β_3-AR agonist CL-316243 (10 μM) were added using FLEX Station fluidics. Subsequent changes in fluorescence were monitored. Mean changes in fluorescence ± SE from 48 wells on a representative plate from 3 independent experiments are shown. Baseline fluorescence was subtracted by instrument software.

To test whether the rat β_3-AR can couple to G_αi and determine its relative coupling efficiency to G_αs and G_αi, CHO cells stably expressing the rat β_3-AR and transiently transfected with empty vector, G_αq/s, or G_αq/i were monitored after addition of 10 μM CL-316243 to the respective cells. In G_αq/s-transfected cells, the agonist produced a rapid mobilization of $Ca^{2+}{}_i$ (Fig. 5), which decayed progressively to 4,000- to 5,000-fold fluorescence units over basal in the 2 min following agonist addition. The rat β_3-AR also coupled to G_αq/i and mobilized $Ca^{2+}{}_i$ in similar rapid fashion after addition of agonist, but in this case the increase averaged 3,000 relative fluorescence units over basal in replicate experiments (Fig. 5). A time-dependent decay from peak $Ca^{2+}{}_i$ was observed in these cells to ~2,000 units over basal. Addition of CL-316243 had no effect on mobilization of $Ca^{2+}{}_i$ in β_3-AR-expressing CHO cells transfected with empty vector (not shown). In separate control experiments, recordings from CHO cells transfected with the G protein chimeras alone showed stable baselines and no response to addition of the β_3-AR agonist (not shown). Collectively, these experiments establish that the rat β_3-AR functionally couples to the G_αq/s chimera in an agonist-dependent manner and produces a robust mobilization of $Ca^{2+}{}_i$. The results show that the G_αq/i chimera can also couple the rat β_3-AR to mobilization of $Ca^{2+}{}_i$, although the efficiency of the coupling is only 30% of the response with G_αq/s (Fig. 5).

Comparison of mouse β_{3A}-AR and β_{3B}-AR coupling to G_αs vs. G_αi using digital video microscopy. Measurement of agonist-induced $Ca^{2+}{}_i$ mobilization with the FLEX Station pro-

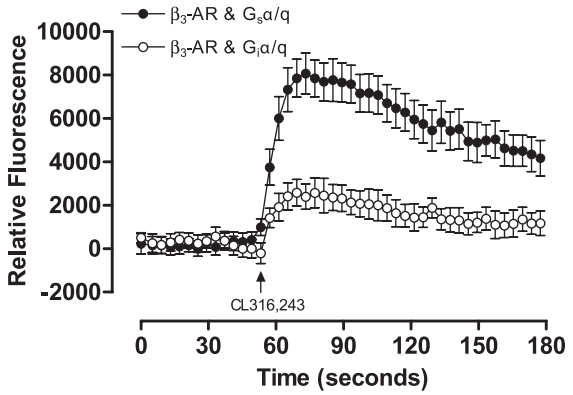

Fig. 5. Receptor-dependent mobilization of $Ca^{2+}{}_i$ in CHO cells stably transformed with rat β_3-AR and transiently transfected with each G protein chimera ($G_\alpha q$/s or $G_\alpha q$/i) or empty vector. Cells stably transformed with rat β_3-AR were transiently transfected with the $G_\alpha q$/s chimera (●), the $G_i\alpha$/q chimera (○), or empty vector (not shown), as described in MATERIALS AND METHODS. Cells from each condition were plated onto 96-well black plates at a seeding density of 80,000 cells/well. Next morning, cells were preloaded for 90 min with the FLIPR calcium assay kit. Plates were placed in the 37°C chamber of the FLEX station and stable baseline recordings obtained as described in MATERIALS AND METHODS. Excitation fluorescence was 485 nm, and emission was detected at 520 nm with 515-nm emission cutoff filter. Buffer control or β_3-AR agonist CL-316243 (10 μM) was added using Flex Station fluidics. Subsequent changes in fluorescence were monitored and baseline fluorescence subtracted by instrument software. Mean changes in fluorescence ± SE from 8 wells on a representative plate from 3 independent experiments are shown.

vides the composite response of a sampled population of cells on the plate. To examine temporal patterns of $Ca^{2+}{}_i$ mobilization in individual cells, we developed an imaging approach to measure agonist-dependent changes in Fluo 3 fluorescence in cells transfected with each combination of mouse β_3-AR splice variant and G protein chimera. Cells were also cotransfected with an expression construct for red fluorescent protein (DsRed) so that recordings were taken from identified, successfully transfected cells. On the basis of previous reports showing that the kinetics and temporal patterns of $Ca^{2+}{}_i$ mobilization (e.g., oscillations vs. monotonic) are agonist concentration dependent (1, 22, 41), initial studies were conducted with CHO cells stably transformed with the M1-CHO to establish how incremental receptor activation is translated with our detection system in this cell type. A saturating concentration of carbachol (10 μM) evoked a large, fourfold increase in $Ca^{2+}{}_i$ followed by a fast and then slow decline of $Ca^{2+}{}_i$ over the following 4 min (Fig. 6*A*). All cells in the viewing field responded simultaneously, so it was necessary to plate cells at low density to resolve and record from individual cells. This dose of carbachol produced a mean maximal increase in relative fluorescence over basal fluorescence of 382.2 ± 35.5% (Fig. 6*A*). A similar pattern of $Ca^{2+}{}_i$ mobilization was also produced with 1 μM and 100 nM carbachol (not shown), but at 10 nM the initial maximal increase in $Ca^{2+}{}_i$ was about twofold lower than the response with 10 μM carbachol (Fig. 6, *A* and *B*). The response to 10 nM carbachol also differed in that after the initial peak $Ca^{2+}{}_i$ decreased and increased in an oscillatory manner. On the basis of our recent work, we attribute this oscillatory pattern to an interplay between calcium release-reuptake mechanisms (22). Treatment of cells with a threshold dose of 1 nM carbachol produced a rapid mobilization of $Ca^{2+}{}_i$ followed by an oscillatory pattern of change in $Ca^{2+}{}_i$ (Fig. 6*C*). This concentration of carbachol produced a maximal increase in $Ca^{2+}{}_i$ of 168 ± 12% with a peak duration of 30 ± 4 s, but after each peak $Ca^{2+}{}_i$ returned to the baseline observed prior to initial agonist treatment (Fig. 6*C*). The oscillatory rise and fall in $Ca^{2+}{}_i$ had intervals between the peaks of ~2 min, and the peaks showed a gradual decline in magnitude of the peak signal (Fig. 6*C*). The results indicate that progressive, agonist-dependent increases in M1-CHO/$G_\alpha q$ coupling transform the temporal pattern of $Ca^{2+}{}_i$ mobilization from a purely oscillatory

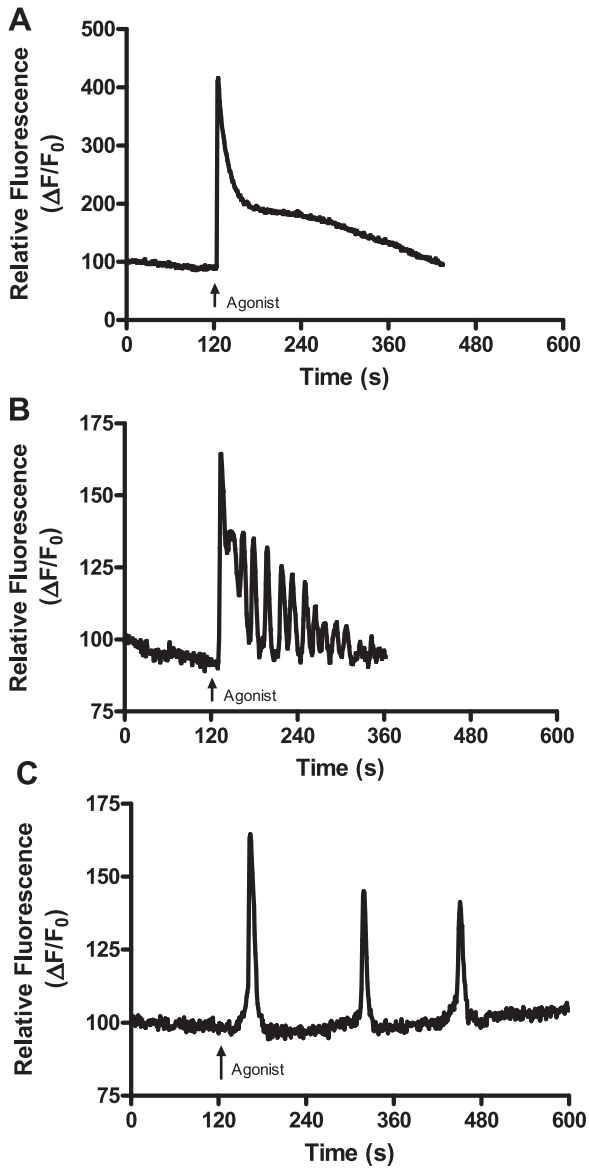

Fig. 6. Receptor-dependent mobilization of $Ca^{2+}{}_i$ in CHO cells stably transformed with M1 muscarinic receptor and treated with 10 μM (*A*), 10 nM (*B*), or 1 nM (*C*) carbachol. CHO cells stably transformed with M1 muscarinic receptor were seeded into single culture dishes and loaded with Fluo 3-AM the next morning as described in MATERIALS AND METHODS. After establishment of stable baseline fluorescence, 10 μM, 10 nM, or 1 nM carbachol was added at 120 s and agonist-dependent fluorescence measured for another 5–10 min. Physically separated cells (6–8) were identified within each field of view and relative change in fluorescence within each cell quantitated and processed by Metamorph software and exported to GraphPad Prism for analysis. Recordings from 6–8 cells in each of 3 experiments were analyzed, and a representative trace is shown.

pattern to a monotonic, biphasic decay pattern with full coupling. Although intermediate levels of agonist produced an intermediate pattern containing elements of both response types (Fig. 6*B*), and although a comprehensive dose-response series was not conducted, the results argue that the progression of response patterns is a reflection of incremental recruitment of $G_\alpha q$ to liganded receptor.

The present evaluation of coupling of β_3-AR splice variants to $G_\alpha s$ and $G_\alpha i$ used a saturating dose of receptor agonist and assessed the recruitment and activation of the $G_\alpha q$ component of each chimera ($G_\alpha q/s$ and $G_\alpha q/i$) based on the magnitude and pattern of calcium mobilization. As reported earlier in RESULTS, initial studies established that our transfection protocol with β_{3A}-AR and β_{3B}-AR resulted in equivalent receptor expression, as judged by measurements of receptor binding and agonist-dependent coupling to endogenous $G_\alpha s$ in both intact cells and cell membranes. A second important control was to show that our transfection protocol with β_{3A}-AR, β_{3B}-AR, and the G protein chimeras produced equivalent coupling of each receptor splice variant to the $G_\alpha q/s$ chimera. The temporal patterns of CL-316243-dependent mobilization of $Ca^{2+}{}_i$ in CHO cells transfected with $G_\alpha q/s$ and β_{3A}-AR or β_{3B}-AR were heterogeneous for each receptor (Fig. 7). In ~30% of cells transfected with each receptor and $G_\alpha q/s$, the agonist produced a single rapid increase in $Ca^{2+}{}_i$ followed by a monophasic decline to basal calcium over the next 3–4 min (Fig. 7, *A* and *B*). The peak amplitude and temporal patterns of decay were similar to the response seen with the highest dose of carbachol in M1-CHO cells (Fig. 6*A*), and the responses did not differ between β_{3A}-AR- and β_{3B}-AR-transfected cells (Fig. 7, *A* and *B*). The remaining 70% of cells transfected with $G_\alpha q/s$ and the β_3-AR splice variants responded to CL-316243 in an oscillatory manner (Fig. 7, *C* and *D*) that was similar to the response observed with low agonist levels in M1-CHO cells (Fig. 6*C*). Cells responding to agonist with either the monotonic or oscillatory pattern of calcium mobilization were typically both found on the same plate, and cells displaying the two response types showed no consistent differences in DsRed expression. The estimates of frequency of the two response types were based on analysis of 6–8 cells per plate and 8–10 plates per receptor splice variant. It was particularly interesting that no intermediate patterns of calcium mobilization, like those produced with 10 nM carbachol in M1-CHO cells, were observed with either β_3-AR splice variant. The underlying reasons are unclear, although experiments with lower, nonsaturating concentrations of receptor agonist may have produced the intermediate pattern within the subpopulation of cells responding with monotonic responses.

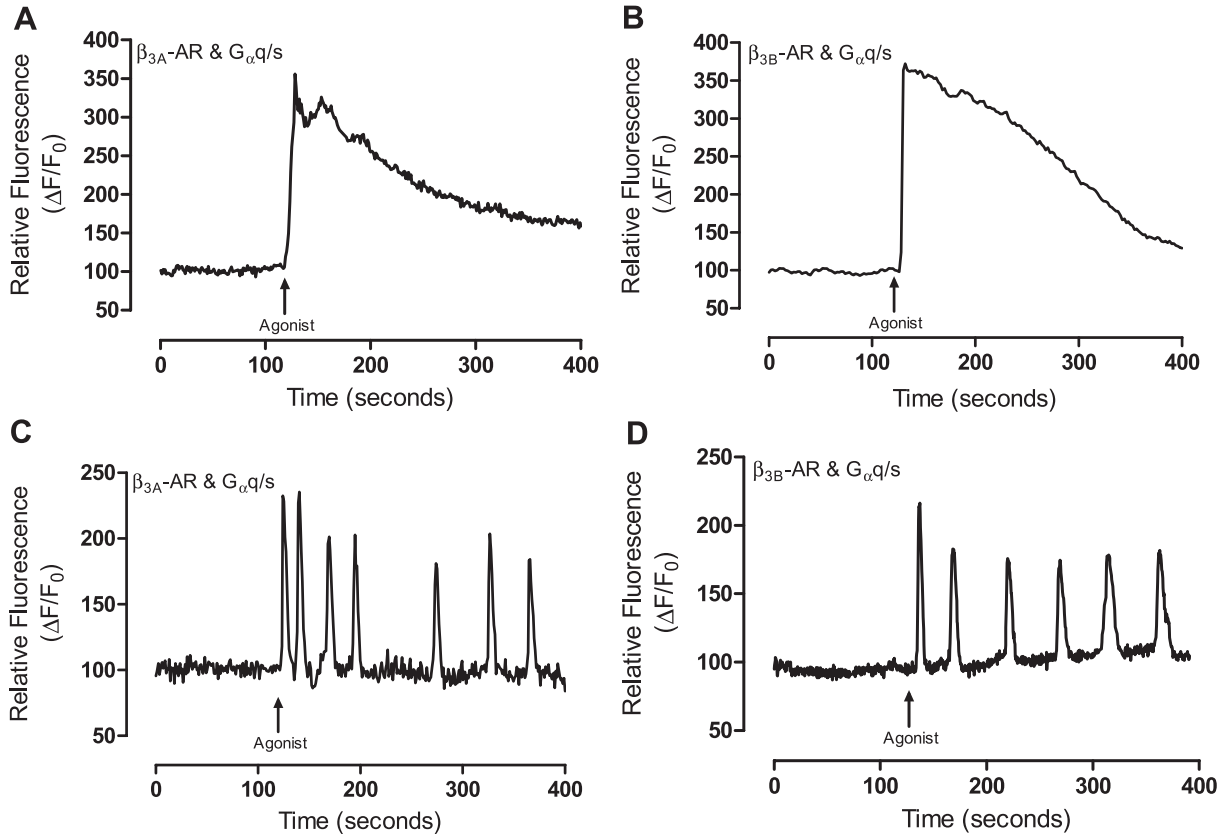

Fig. 7. Receptor-dependent mobilization of $Ca^{2+}{}_i$ in CHO cells transiently transfected with mouse β_{3A}-AR (*A* and *C*) or β_{3B}-AR (*B* and *D*) and $G_\alpha q/s$ chimeras. CHO cells were transiently transfected for 16 h with each combination of receptor isoform and $G_\alpha q/s$, with an expression construct for red fluorescent protein (DsRed), as described in MATERIALS AND METHODS. After 16 h, cells were loaded with Fluo 3-AM, and cells expressing DsRed fluorescence were identified and used for analysis of agonist-dependent calcium mobilization. After establishment of stable baseline fluorescence of Fluo 3 in physically separated DsRed-positive cells, 10 μM CL-316243 were added at 120 s and agonist-dependent fluorescence was measured for a further 3–4 min. Relative change in fluorescence within each cell was quantitated and processed by Metamorph software and exported to GraphPad Prism for analysis as described in MATERIALS AND METHODS. Recordings from 6–8 cells in each of 3 experiments were analyzed, and a representative trace is shown from cells transfected with each receptor isoform that responded with monotonic (*A* and *B*) or oscillatory (*C* and *D*) patterns of calcium mobilization.

To objectively compare the oscillatory responses between the subpopulations of cells transfected with each receptor splice variant, the temporal patterns of calcium mobilization were analyzed by comparing peak amplitude, peak duration, and interval between peaks. In the subpopulation of cells showing the oscillatory response to agonist, no evidence was found to support the hypothesis that the peak amplitude ($P > 0.05$), peak duration ($P > 0.05$), or interval between peaks ($P > 0.05$) differed between receptor splice variants coupled with $G_\alpha q/s$ (Fig. 7, *C* and *D*). And although not shown, the parameter estimates for the rat β_3-AR were similar to those obtained with the mouse receptors. CHO cells stably transformed with the 5-HT_{1A} serotonin receptor and transfected with $G_\alpha q/i$ were used as a positive control for $G_\alpha i$-preferring receptors. Treatment of cells with 10 μM serotonin produced both monotonic and oscillatory patterns of calcium mobilization with peak amplitudes and durations similar to those observed with β_3-ARs and $G_\alpha q/s$ (data not shown).

In contrast, in cells transfected with $G_\alpha q/i$ and β_3-AR splice variants, 100% of the cells examined responded to agonist with an oscillatory pattern of calcium mobilization (Fig. 8). The peak amplitude observed in cells transfected with β_{3A}-AR (223 ± 11 relative fluorescence units) and β_{3B}-AR (227 ± 8 relative fluorescence units) did not differ, and the peak duration (β_{3A}-AR 30 ± 1.3 s, β_{3B}-AR 31 ± 1.4 s) and interval (β_{3A}-AR 151 ± 7.3 s, β_{3B}-AR 156 ± 5.3 s) were also comparable. Collectively, the analysis shows that the two receptor splice variants produced equivalent patterns of calcium mobilization and provides no evidence that the two receptors couple differently from $G_\alpha i$.

Using data from the single-cell imaging approach to provide a quantitative assessment of relative coupling of β_{3A}-AR and β_{3B}-AR to $G_\alpha s$ vs. $G_\alpha i$ is complicated by the heterogeneity of responses with $G_\alpha q/s$ (see Fig. 7). When peak amplitude is the basis for comparison, analysis of variance provides no evidence of a receptor isoform × G protein interaction ($P > 0.05$) or differences in response attributable to receptor isoform ($P > 0.05$). However, differences in response between G proteins, averaged across receptor isoform, were significant ($P < 0.01$) and accounted for the majority of variance among the groups. The absence of monotonic patterns of calcium mobilization in cells transfected with $G_\alpha q/i$ and the lower average peak amplitudes, compared with $G_\alpha q/s$, are consistent with more effective β_3-AR coupling to $G_\alpha q/s$. The differences were more subtle when the analysis was restricted to a comparison of $G_\alpha q/s$- or $G_\alpha q/i$-transfected cells that responded with an oscillatory pattern of calcium mobilization. For instance, peak amplitude did not differ between $G_\alpha q/s$ and $G_\alpha q/i$ (Fig. 7, *C* and *D*, vs. Fig. 8, *A* and *B*). However, the intervals between peaks were significantly longer ($P < 0.05$) in cells transfected with $G_\alpha q/i$ (β_{3A}-AR 151 ± 21 s, β_{3B}-AR 156 ± 5 s) than with $G_\alpha q/s$ (β_{3A}-AR 40 ± 9 s, β_{3B}-AR 41 ± 10 s), irrespective of the receptor splice variant. This translates into fewer peaks per unit time with $G_\alpha q/i$ vs. $G_\alpha q/s$ and significantly less calcium mobilization in response to receptor activation. Although this analysis does not provide a quantitative measurement of the relative coupling of the β_3-AR splice variants to $G_\alpha q/s$ vs. $G_\alpha q/i$, the data support a significant albeit less effective coupling of each receptor to $G_\alpha q/i$ than to $G_\alpha q/s$. Moreover, this finding is consistent with conclusions reached independently using the high-throughput approach with the rat β_3-AR and G protein chimeras.

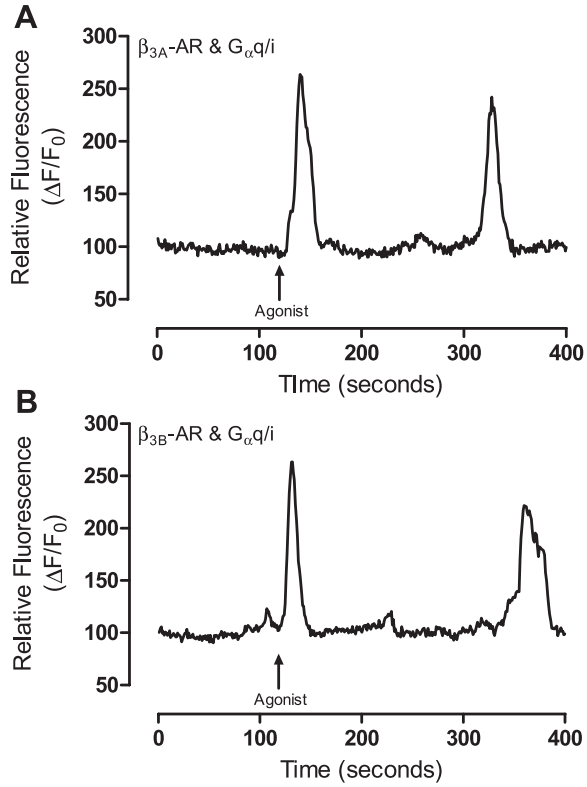

Fig. 8. Receptor-dependent mobilization of $Ca^{2+}{}_i$ in CHO cells transiently transfected with mouse β_{3A}-AR (*A*) or β_{3B}-AR (*B*) and the $G_\alpha q/i$ chimera. CHO cells were transiently transfected for 16 h with each receptor isoform, the $G_\alpha q/i$ chimera, and the expression construct for DsRed as described in MATERIALS AND METHODS. After 16 h, cells were loaded with Fluo 3-AM, and cells expressing DsRed fluorescence were identified and used for analysis of agonist-dependent calcium mobilization. After establishment of stable baseline fluorescence of Fluo 3 in physically separated DsRed-positive cells, 10 μM CL-316243 were added at 120 s and agonist-dependent fluorescence was measured for another 3–4 min. Relative change in fluorescence within each cell was quantitated and processed by Metamorph software and exported to GraphPad Prism for analysis as described in MATERIALS AND METHODS. Recordings from 6–8 cells in each of 3 experiments were analyzed, and a representative trace is shown from cells transfected with each receptor isoform.

DISCUSSION

Many receptors are known to be promiscuous in the sense that they couple with more than one class of G protein α-subunit (11, 16, 33, 42). In such cases, receptor activation produces a complex array of signals to effector systems that translate the response to agonist in a given cell context. Previous work provided indirect evidence that the β_3-AR coupled to both $G_\alpha s$ and $G_\alpha i$ in rat adipocytes (4). The authors resolved the dual interaction by blocking receptor coupling to $G_\alpha i$ with PTX, and showing enhanced signaling through $G_\alpha s$ (4). Using a GTP photoaffinity probe, Soeder et al. (40) showed that a β_3-AR agonist increased binding of AA-GTP to proteins migrating at 40–42 kDa and presumed to be $G_\alpha i$ in membranes from rat white adipocytes. The rationale for the present work stems from work by Evans et al. (13, 23), showing that alternative splicing of the mouse β_3-AR gene produced two isoforms (β_{3A}-AR and β_{3B}-AR) that differ in

their COOH-terminal sequence and ability to couple to $G_\alpha i$. They found that the β_{3B}-AR, but not the β_{3A}-AR, could activate $G_\alpha i$. Particularly interesting was their finding of tissue-specific expression ratios of the splice variants beween BAT and WAT (13), where it was reported that mRNA coding for the β_{3B}-AR represented 21% of total β_3-AR transcripts in WAT but only 7% in BAT. Although it is unclear whether the encoded proteins are expressed in similar ratios, the predicted paucity of β_{3B}-AR expression in BAT relative to WAT could produce tissue-specific translations of agonist input if the β_{3A}-AR coupled only with $G_\alpha s$ (23, 39). For example, β_3-ARs activate MAPK through $G_\alpha i$ in several (3, 40) but not all (34) white adipocyte cell lines, whereas the evidence supports a $G_\alpha s$-cAMP-PKA-dependent pathway not involving $G_\alpha i$ in primary cultures of brown adipocytes (31). Whether these differences are linked to differential expression of the β_{3B}-AR between brown and white adipocytes has not been resolved. However, understanding the respective signaling pathways engaged by norepinephrine in each cell type represents a key point in understanding how sympathetic input will be translated in BAT and WAT.

Evidence that β_{3A}-AR and β_{3B}-AR differentially couple to $G_\alpha i$ is based on observed differences in agonist-dependent increases in cAMP after PTX treatment of cells expressing each receptor isoform (23). For example, PTX enhanced agonist-dependent increases in cAMP in cells expressing the β_{3B}-AR but not the β_{3A}-AR, the inference being that the net increase in cAMP was a measure of β_{3B}-AR- but not β_{3A}-AR-dependent activation of $G_\alpha i$ (23). By use of this approach, the $G_\alpha i$ component of receptor input into adenylyl cyclase activity is measured indirectly as the net change in cAMP in the presence and absence of PTX and assumes that receptor input through $G_\alpha s$ is unchanged. To provide a direct measurement of β_3-AR coupling to $G_\alpha i$ in the absence of prior assumptions regarding its coupling to $G_\alpha s$, we developed two independent approaches to provide direct assessments of the relative ability of the mouse β_3-AR isoforms and the rat β_3-AR to activate $G_\alpha i$ in an agonist-dependent manner. The first approach used expression constructs for G protein chimeras in conjunction with the receptor isoforms to *1*) assess the relative coupling of β_3-ARs to $G_\alpha i$ vs. $G_\alpha s$ and *2*) determine whether β_{3A}-AR and β_{3B}-AR splice variants differentially couple to $G_\alpha i$. This general approach was developed by Conklin and Bourne (6) as part of an effort to identify specific receptor/G protein contact sites responsible for conferring signaling specificity (32). Although additional points of contact are involved in the physical interaction between receptor and G protein, the COOH-terminal heptapeptide is the key structural element that determines the specificity of receptor/G protein interaction (27). By mutating residues within this region of $G_\alpha q$ to match the heptapeptide sequences of $G_\alpha s$ or $G_\alpha i$, those authors produced chimeric G proteins that effectively transformed the response to receptor activation from regulation of adenylyl cyclase to activation of phospholipase C and mobilization of $Ca^{2+}{}_i$ (7–9, 32). Using both a high-throughput fluorometric imaging platform and a single-cell-based imaging approach, we found that *1*) β_3-ARs are approximately threefold more effective in activating $G_\alpha s$ than $G_\alpha i$, and *2*) β_{3A}- and β_{3B}-AR splice variants are equally effective in activating $G_\alpha i$.

The second independent approach used to assess β_3-AR coupling to $G_\alpha i$ measured ligand-dependent binding of the photoreactive GTP analog, 4-azidoanilido-[α-^{32}P]-GTP (AA-GTP) in plasma membranes from CHO cells stably transformed with the rat β_3-AR. The rat β_3-AR is highly homologous (~95%) to the mouse β_{3A}-AR (see Fig. 1) and produced a threefold increase in AA-GTP binding to $G_\alpha i$ in a ligand-dependent manner. A cell line expressing the canonical $G_\alpha i$-coupled 5-HT_{1A} receptor provided a positive control and showed a serotonin-dependent five- to sixfold increase in AA-GTP binding to the 41-kDa proteins that we identified previously as $G_\alpha i$-2 and $G_\alpha i$-3 (16). Thus our findings with the rat β_3-AR are consistent using both approaches and support the conclusion that this receptor activates $G_\alpha i$ in a ligand-dependent manner.

The COOH terminus of many receptors contains ubiquitous protein interaction modules (PDZ domains) that sequester proteins that modify G protein coupling and receptor recycling (36, 43, 44). Although a consensus PDZ domain is not evident in the COOH terminus of mouse β_{3A}-AR, recent work provided evidence that protein-protein interactions with the β_{3A}-AR COOH terminus were the basis for its inability to interact with $G_\alpha i$ (39) in CHO cells. Preincubation with a membrane-permeable peptide corresponding to the COOH terminus of β_{3A}-AR conferred PTX sensitivity to agonist-mediated increases in cellular cAMP (39), suggesting that interaction of an endogenous protein with the COOH terminus of β_{3A}-AR prevented its coupling to $G_\alpha i$. If this hypothesis is correct, we predict that preincubation with the peptide should enhance β_{3A}-AR/$G_\alpha i$ interaction and reduce agonist-dependent increases in cAMP.

With both the mouse β_{3A}-AR and its rat β_{3A}-AR homolog, we find no evidence of an impaired ability of this receptor isoform to interact with $G_\alpha i$ in an agonist-dependent manner. The fundamental difference between the present and previous findings (23, 39) on this point are likely rooted in experimental approach. The PTX approach measures the strength of the β_3-AR/$G_\alpha i$ interaction as a net change (23) in adenylyl cyclase activation and makes the implicit assumption that PTX effects on this response are limited to ADP ribosylation of $G_\alpha i$. Although PTX does prevent receptor-$G_\alpha i$ coupling, it has a number of additional effects, including activation of ERK1/2 through a novel pathway (15), activation of the Toll-like receptor 4 (25), and activation of tyrosine kinases (28). Moreover, the catalytically inactive β-oligomer of PTX was shown to activate NF-κB and alter receptor trafficking to the membrane (24). It is evident that these effects of PTX have the potential to alter cell function and confound experimental outcomes. In contrast, the two approaches that we took involved direct readouts of G protein activation by the β_3-AR isoforms. This was accomplished in the first approach with G protein chimeras, which translated receptor-dependent G protein activation into mobilization of $Ca^{2+}{}_i$. Therefore, rather than β_3-AR-mediated activation of $G_\alpha s$ and $G_\alpha i$ converging on a single effector system (i.e., adenylyl cyclase) and assessment of relative input based on subtraction, the chimeric transformation of the readout provided independent measurements of receptor-dependent input to $G_\alpha s$ and $G_\alpha i$. A limitation of this approach is that assembly of protein complexes important to signal integration differs among G proteins, and the G protein chimeras would be expected to form protein complexes similarly to $G_q\alpha$ rather than $G_\alpha i$ and $G_\alpha s$. This difference has the potential to allow receptor-G protein interactions that might not

normally occur. However, our finding that the rat β_3-AR produced a threefold, agonist-dependent increase in AA-GTP binding to endogenous $G_\alpha i$ is consistent with our findings using the chimeras and argues against artifactual receptor-G protein interactions based on the novel structure of the chimeras. It has also become evident that scaffolding and accessory proteins regulate signal processing by recruiting regulatory elements such as activators of G protein signaling family members to receptor-G protein signaling complexes (36, 43, 44). This represents an additional limitation of the present studies in that the assessment of effector system regulation reflects the unique signaling environment of CHO cells. Therefore, it will be important in future studies to evaluate how the relevant cellular environment of the adipocyte influences the interaction of β_3-AR splice variants with G protein subtypes.

Notwithstanding these caveats, our results also show that β_3-ARs couple less efficiently to $G_\alpha q/i$ vs. $G_\alpha q/s$. Attempts were made to compare coupling efficiency of the rat β_3-AR to endogenous $G_\alpha i$ vs. $G_\alpha s$ using AA-GTP, but significant differences in the Mg^{2+} concentrations required for optimal binding of AA-GTP to $G_\alpha i$ (μM) vs. $G_\alpha s$ (mM) prevented an objective assessment with this approach (14). Collectively, our findings indicate that the COOH-terminal sequences produced by alternative splicing of the mouse β_3-AR gene are not critical determinants for interaction with $G_\alpha i$ or $G_\alpha s$ and do not contain the structural features that convey the relative preference of β_3-ARs for $G_\alpha s$ over $G_\alpha i$. We estimate that β_3-ARs coupled to $G_\alpha i$ will evoke only one-third the response produced when they couple to $G_\alpha s$. However, this calculation may be influenced by the relative stoichiometry and G protein subtype expression profiles of the cell line being evaluated (18, 38). For instance, the high levels of $G_\alpha i$ subtype ($G_\alpha i$-1, $G_\alpha i$-2, $G_\alpha i$-3) expression in the adipocyte (18), relative to $G_\alpha s$, could enhance the impact of β_3-AR-dependent $G_\alpha i$ activation and have important effects on translation of catecholaminergic input in adipose tissue.

ACKNOWLEDGMENTS

We gratefully acknowledge the generosity of our colleagues who shared expression constructs for the rat β_3-AR (Dr. J. Granneman, Wayne State University, Detroit, MI), the mouse β_{3A}- and β_{3B}-AR (Dr. R. Summers, Monash University, Victoria, Australia), and the $G_\alpha q/s$ and $G_\alpha q/i$ chimeras (Dr. B. Conklin, Scripps, San Diego, CA). We also thank Dr. J. Raymond (Medical University of South Carolina, Charleston, SC) for CHO cells stably transformed with the 5-HT_{1A} receptor.

GRANTS

This work was supported by National Institute of Diabetes and Digestive and Kidney Diseases (NIDDK) Grants DK-53872 (T. W. Gettys), DK-06156 (T. W. Gettys), and DK-052142 (R. C. Rogers) and by a research grant from the American Diabetes Association (T. W. Gettys). A. W. Adamson is supported by NIDDK Training Grant T32-DK-064584-02. N. R. Lenard is the recipient of an individual National Research Service Award (F32-DA-18028).

REFERENCES

1. **Akagi K, Nagao T, and Urushidani T.** Calcium oscillations in single cultured Chinese hamster ovary cells stably transfected with a cloned human cholecystokinin (CCK)B receptor. *Jpn J Pharmacol* 75: 33–42, 1997.
2. **Benovic JL, Pike LJ, Cerione RA, Staniszewiski C, Yoshimasa T, Codina J, Caron MG, and Lefkowitz RJ.** Phosphorylation of the mammalian beta-adrenergic receptor by cyclic AMP-dependent protein kinase. *J Biol Chem* 260: 7094–7101, 1985.
3. **Cao WH, Luttrell LM, Medvedev AV, Pierce KL, Daniel KW, Dixon TM, Lefkowitz RJ, and Collins S.** Direct binding of activated c-Src to the β_3-adrenergic receptor is required for MAP kinase activation. *J Biol Chem* 275: 38131–38134, 2000.
4. **Chaudhry A, MacKenzie RG, Georgic LM, and Granneman JG.** Differential interaction of β_1- and β_3-adrenergic receptors with G_i in rat adipocytes. *Cell Signal* 6: 457–465, 1994.
5. **Commins SP, Watson PM, Levin N, Beiler RJ, and Gettys TW.** Central leptin regulates the *UCP1* and *ob* genes in brown and white adipose tissue via different β-adrenoceptor subtypes. *J Biol Chem* 275: 33059–33067, 2000.
6. **Conklin BR and Bourne HR.** Structural elements of Gα subunits that interact with Gβγ, receptors, and effectors. *Cell* 73: 631–641, 1993.
7. **Conklin BR, Farfel Z, Lustig KD, Julius D, and Bourne HR.** Substitution of three amino acids switches receptor specificity of $G_q\alpha$ to that of $G_i\alpha$. *Nature* 363: 274–276, 1993.
8. **Conklin BR, Herzmark P, Ishida S, Voyno-Yasenetskaya TA, Sun Y, Farfel Z, and Bourne HR.** Carboxyl-terminal mutations of $G_{q\alpha}$ and $G_{s\alpha}$ that alter the fidelity of receptor activation. *Mol Pharmacol* 50: 885–890, 1996.
9. **Coward P, Chan SD, Wada HG, Humphries GM, and Conklin BR.** Chimeric G proteins allow a high-throughput signaling assay of Gi-coupled receptors. *Anal Biochem* 270: 242–248, 1999.
10. **Daaka Y, Luttrell LM, and Lefkowitz RJ.** Switching of the coupling of the β_2-adrenergic receptor to different G proteins by protein kinase A. *Nature* 390: 88–91, 1997.
11. **Eason MG, Kurose H, Holt BD, Raymond JR, and Liggett SB.** Simultaneous coupling of α_2-adrenergic receptors to two G-proteins with opposing effects. Subtype-selective coupling of α_2C10, α_2C4, and α_2C2 adrenergic receptors to G_i and G_s. *J Biol Chem* 267: 15795–15801, 1992.
12. **Emorine LJ, Marullo S, Briend-Sutren MM, Patey G, Tate K, avier-Klutchko C, and Strosberg AD.** Molecular characterization of the human beta 3-adrenergic receptor. *Science* 245: 1118–1121, 1989.
13. **Evans BA, Papaioannou M, Hamilton S, and Summers RJ.** Alternative splicing generates two isoforms of the β3-adrenoceptor which are differentially expressed in mouse tissues. *Br J Pharmacol* 127: 1525–1531, 1999.
14. **Fields TA, Linder ME, and Casey PJ.** Subtype-specific binding of azidoanilido-GTP by purified G protein alpha subunits. *Biochemistry* 33: 6877–6883, 1994.
15. **Garcia JG, Wang P, Liu F, Hershenson MB, Borbiev T, and Verin AD.** Pertussis toxin directly activates endothelial cell p42/p44 MAP kinases via a novel signaling pathway. *Am J Physiol Cell Physiol* 280: C1233–C1241, 2001.
16. **Gettys TW, Fields TA, and Raymond JR.** Selective activation of inhibitory G protein alpha-subunits by partial agonists of the human 5-HT1A receptor. *Biochemistry* 33: 4283–4290, 1994.
17. **Gettys TW, Okonogi K, Tarry WC, Johnston J, Horton C, and Taylor IL.** Examination of relative rates of cAMP synthesis and degradation in crude membranes of adipocytes treated with hormones. *Second Messengers and Phosphoproteins* 13: 37–50, 1990.
18. **Gettys TW, Sheriff-Carter K, Moomaw J, Taylor IL, and Raymond JR.** Characterization and use of crude alpha-subunit preparations for quantitative immunoblotting of G proteins. *Anal Biochem* 220: 82–91, 1994.
19. **Gettys TW, Watson PM, Seger L, Padgett M, and Taylor IL.** Adrenalectomy after weaning restores β_3-adrenergic receptor expression in white adipocytes from C57BL/6J mice. *Endocrinology* 138: 2697–2704, 1997.
20. **Granneman JG, Lahners KN, and Chaudhry A.** Molecular cloning and expression of the rat β3-adrenergic receptor. *Mol Pharmacol* 40: 895–899, 1991.
21. **Granneman JG, Lahners KN, and Rao DD.** Rodent and human beta 3-adrenergic receptor genes contain an intron within the protein-coding block. *Mol Pharmacol* 42: 964–970, 1992.
22. **Hermann GE, Nasse JS, and Rogers RC.** Alpha-1 adrenergic input to solitary nucleus neurones: calcium oscillations, excitation and gastric reflex control. *J Physiol* 562: 553–568, 2005.
23. **Hutchinson DS, Bengtsson T, Evans BA, and Summers RJ.** Mouse β3A- and β3B-adrenoceptors expressed in chinese hamster ovary cells display identical pharmacology but utilize distinct signalling pathways. *Br J Pharmacol* 135: 1903–1914, 2002.
24. **Jajoo S, Mukherjea D, Pingle SC, Sekino Y, and Ramkumar V.** Induction of adenosine A1 receptor expression by pertussis toxin via an ADP ribosylation independent pathway. *J Pharmacol Exp Ther* 317: 1–10, 2006.

25. **Kerfoot SM, Long EM, Hickey MJ, Andonegui G, Lapointe BM, Zanardo RC, Bonder C, James WG, Robbins SM, and Kubes P.** TLR4 contributes to disease-inducing mechanisms resulting in central nervous system autoimmune disease. *J Immunol* 173: 7070–7077, 2004.
26. **Konkar AA, Zhai Y, and Granneman JG.** β1-Adrenergic receptors mediate β3-adrenergic-independent effects of CGP 12177 in brown adipose tissue. *Mol Pharmacol* 57: 252–258, 2000.
27. **Kostenis E, Conklin BR, and Wess J.** Molecular basis of receptor/G protein coupling selectivity studied by coexpression of wild type and mutant m2 muscarinic receptors with mutant Galphaq subunits. *Biochemistry* 36: 1487–1495, 1997.
28. **Li H and Wong WS.** Pertussis toxin activates tyrosine kinase signaling cascade in myelomonocytic cells: a mechanism for cell adhesion. *Biochem Biophys Res Commun* 283: 1077–1082, 2001.
29. **Liggett SB, Bouvier M, Hausdorff WP, O'Dowd B, Caron MG, and Lefkowitz RJ.** Altered patterns of agonist-stimulated cAMP accumulation in cells expressing mutant beta 2-adrenergic receptors lacking phosphorylation sites. *Mol Pharmacol* 36: 641–646, 1989.
30. **Liggett SB, Freedman NJ, Schwinn DA, and Lefkowitz RJ.** Structural basis for receptor subtype-specific regulation revealed by a chimeric beta 3/beta 2-adrenergic receptor. *Proc Natl Acad Sci USA* 90: 3665–3669, 1993.
31. **Lindquist JM, Fredriksson JM, Rehnmark S, Cannon B, and Nedergaard J.** β_3- and α_1-adrenergic Erk1/2 activation is Src- but not G_i-mediated in brown adipocytes. *J Biol Chem* 275: 22670–22677, 2000.
32. **Liu J, Conklin BR, Blin N, Yun J, and Wess J.** Identification of a receptor/G-protein contact site critical for signaling specificity and G protein activation. *Proc Natl Acad Sci USA* 92: 11646, 1995.
33. **Macnulty EE, McClue SJ, Carr IC, Jess T, Wakelam MJ, and Milligan G.** Alpha-2-C10 adrenergic receptors expressed in rat 1 fibroblasts can regulate both adenylylcyclase and phospholipase D-mediated hydrolysis of phosphotidylcholine by interacting with pertussis toxin-sensitive guanine nucleotide-binding proteins. *J Biol Chem* 267: 2149–2156, 1992.
34. **Mizuno K, Kanda Y, Kuroki Y, and Watanabe Y.** The stimulation of β_3-adrenoceptor causes phosphorylation of extracellular signal-regulated kinases 1 and 2 through a G_s- but not G_i-dependent pathway in 3T3-L1 adipocytes. *Eur J Pharmacol* 404: 63–68, 2000.
35. **Nahmias C, Blin N, Elalouf J-M, Mattei MG, Strosberg AD, and Emorine LJ.** Molecular characterization of the mouse β3-adrenergic receptor: relationship with the atypical receptor of adipocytes. *EMBO J* 10: 3721–3727, 1991.
36. **Ranganathan R and Ross EM.** PDZ domain proteins: scaffolds for signaling complexes. *Curr Biol* 7: R770–R773, 1997.
37. **Raymond JR, Arthur JM, Casanas SJ, Olsen CL, Gettys TW, and Mortensen RM.** Alpha-2A adrenergic receptors inhibit cAMP accumulation in embryonic stem cells which lack Gi-alpha-2. *J Biol Chem* 269: 13073–13075, 1994.
38. **Raymond JR, Olsen CL, and Gettys TW.** Cell-specific physical and functional coupling of human 5-HT1A receptors to inhibitory G protein alpha-subunits and lack of coupling to Gs-alpha. *Biochemistry* 32: 11064–11073, 1993.
39. **Sato M, Hutchinson DS, Bengtsson T, Floren A, Langel U, Horinouchi T, Evans BA, and Summers RJ.** Functional domains of the mouse beta3-adrenoceptor associated with differential G protein coupling. *J Pharmacol Exp Ther* 315: 1354–1361, 2005.
40. **Soeder KJ, Snedden SK, Cao WH, Della R, Daniel KW, Luttrell LM, and Collins S.** The β_3-adrenergic receptor activates mitogen-activated protein kinase in adipocytes through a G_i-dependent mechanism. *J Biol Chem* 274: 12017–12022, 1999.
41. **Somogyi R and Stucki JW.** Hormone-induced calcium oscillations in liver cells can be explained by a simple one pool model. *J Biol Chem* 266: 11068–11077, 1991.
42. **Wong YH, Conklin BR, and Bourne HR.** Gz-mediated hormonal inhibition of cyclic AMP accumulation. *Science* 255: 339–342, 1992.
43. **Xiang Y, Devic E, and Kobilka B.** The PDZ binding motif of the beta 1 adrenergic receptor modulates receptor trafficking and signaling in cardiac myocytes. *J Biol Chem* 277: 33783–33790, 2002.
44. **Xiang Y and Kobilka B.** The PDZ-binding motif of the beta2-adrenoceptor is essential for physiologic signaling and trafficking in cardiac myocytes. *Proc Natl Acad Sci USA* 100: 10776–10781, 2003.